



## Original Article

Measurement of TOF of fast neutrons with  $^{238}\text{U}$  target

Meng Li <sup>a, b</sup>, Yuanfan Guan <sup>a, b</sup>, Chengui Lu <sup>a, b</sup>, Junwei Zhang <sup>c</sup>, Xiaohua Yuan <sup>a, b</sup>,  
Limin Duan <sup>a, b</sup>, Herun Yang <sup>a, b, \*</sup>, Rongjiang Hu <sup>a, b</sup>, Zhiyong He <sup>a, b</sup>, Xianglun Wei <sup>a, b</sup>,  
Peng Ma <sup>a, b</sup>, Zaiguo Gan <sup>a, b</sup>, Chunli Yang <sup>a</sup>, Hongbin Zhang <sup>a</sup>, Liang Chen <sup>a, b</sup>, Tianli Qiu <sup>a, b</sup>,  
Yikai Hou <sup>d</sup>

<sup>a</sup> Institute of Modern Physics, Chinese Academy of Sciences, Lanzhou, 730000, China

<sup>b</sup> School of Nuclear Science and Technology, University of Chinese Academy of Sciences, Beijing, 100049, China

<sup>c</sup> North China University of Water Resources and Electric Power, Zhengzhou, 450000, China

<sup>d</sup> School of Nuclear Science and Technology, Lanzhou University, Lanzhou, 730000, China



## ARTICLE INFO

## Article history:

Received 29 March 2020

Received in revised form

16 November 2020

Accepted 1 December 2020

Available online 13 December 2020

## Keywords:

Parallel plate avalanche counter

The time resolution

Neutron

Time-of-flight(TOF)

## ABSTRACT

We developed a Dual-PPACs detector for fast neutron measurements that consists of two sets of PPAC: conventional PPAC and fission PPAC. A  $^{238}\text{U}(\text{U}_3\text{O}_8)$  coating is placed in the fission PPAC's anode, which is used as the neutrons conversion layer. An experiment was performed to measure neutron time-of-flight (TOF) in which  $^{252}\text{Cf}$  spontaneous fission source was used. An excellent time resolution of 164ps has been observed at 6 mbar in isobutene gas. With the excellent time resolution of Dual-PPACs detector, exact neutron energy can be extracted from the timing measurement. The experimental detection efficiency was  $1.9 \times 10^{-7}$ , consistent with the efficiency of  $2.5 \times 10^{-7}$  given by a Geant4 simulation. Ultimately, the results show that the Dual-PPACs detector is a suitable candidate for measuring fast neutrons in the future CiADS system.

© 2020 Korean Nuclear Society, Published by Elsevier Korea LLC. This is an open access article under the CC BY-NC-ND license (<http://creativecommons.org/licenses/by-nc-nd/4.0/>).

## 1. Introduction

In 2011, the China initiative Accelerator Driven System (CiADS) under the Strategic Priority Research Program was founded by the Chinese Academy of Sciences. In January 2018, the National Development and Reform Commission approved the construction of CiADS in Guangdong province. CiADS consists of an accelerator, a sub-critical reactor, and a spallation target located at the center of the reactor core. Therefore, fast neutron measurements are very important in numerous applications in the future CiADS system. This paper focuses on our parallel plate avalanche counter (PPAC) detector with a  $^{238}\text{U}(\text{U}_3\text{O}_8)$  coating for fast neutron measurements. The first recorded application of the PPAC detector was in 1952 by J. Christiansen. Since around 1975, PPAC detectors were recognized for their superior performance as heavy-ion detectors [1]. Since PPACs have good resolutions in both time and position, they have been widely used to detect heavy ions in nuclear reaction experiments for many years [2–7]. The gas detector group of the Institute

of Modern Physics developed a 2-D position-sensitive PPAC with a large active area working under low gas pressure that could realize real-time beam position monitoring [8].

Moreover, compared with other detectors, PPACs are characterized by position measurement capability, large sensitive area, and absolute gamma-insensitivity, which makes them well suitable for neutron detection. Neutrons, as electrically neutral particles, can't produce ionization or excitation directly along their passage through matter. The essence of neutron detection is to detect the secondary charged particles produced in the interaction between neutron and nucleus. Therefore, the fissionable materials like  $^{238}\text{U}$ ,  $^{242}\text{Pu}$ , or  $^{232}\text{Th}$  are used as a fast neutron converter in neutron detector frequently. While  $^{238}\text{U}$  is relatively abundant in nature than the other two nuclides and easy to obtain, this study utilized fission materials of  $^{238}\text{U}(\text{U}_3\text{O}_8)$  coating as neutron converter. With the excellent time resolution of PPAC, the energy of fast neutrons can be deduced from the time-of-flight (TOF) measurement. Furthermore, our detector is composed of two sets of PPACs. In the neutron flux measurement, one PPAC can be used for neutron flux measurement, while the other can be used for calibration or gamma compensation.

\* Corresponding author. Institute of Modern Physics, Chinese Academy of Sciences, Lanzhou, 730000, China.

E-mail address: [yanghr@impcas.ac.cn](mailto:yanghr@impcas.ac.cn) (H. Yang).

## 2. Design and construction

The PPAC has a sandwich structure which contains two cathodes on both sides and an anode on the center. Fig. 1(b) shows a photograph of the Dual-PPACs we designed to detect fast neutron. As shown in Fig. 1 (a), the PPAC detector consists of 7 layers. Layers 1–3 serve as the conventional PPAC, and layers 5–7 form the fission PPAC that contains the neutron conversion layer; layer 4 is the separator layer of two PPAC. All the electrodes were made of 2 μm double-sided aluminized Mylar foils. The active diameter of the detector is Φ60mm, and the layer spacing is 3 mm. To avoid signal crosstalk, we grounded the fourth layer to separate the two sets of PPAC. Sandwich like anode of the fission PPAC is shown in Fig. 1(c), the U<sub>3</sub>O<sub>8</sub> (<sup>238</sup>U) coating was attached to the central anode of the fission PPAC. Coating layer is protected within two double-sided aluminized Mylar films which are applied the same voltage.

When the fast neutron incidents into the <sup>238</sup>U conversion foil, the greater the thickness of the conversion foil, the greater the probability of reaction, and more charged particles will be produced. However, the charged particles produced at the same time have a certain attenuation distance due to the blocking effect of the conversion body in <sup>238</sup>U solid. Therefore, there is an optimal thickness of <sup>238</sup>U conversion foil in two action games. We performed the simulation with the Geant4 program for the conversion

efficiency of <sup>238</sup>U as the thickness of the neutron converter foil [9,10]. The <sup>252</sup>Cf source is a spontaneous fission neutron source, serves as a suitable candidate to test the designed PPAC detector's performance. The energy distribution of fast neutrons from <sup>252</sup>Cf fission can be described as the Maxwell distribution which peaked at 2.1 MeV in the simulation. In order to optimize the calculation, the actual distance between the detector and the source must be set in the simulation to eliminate the difference between the simulation and experimental condition. The conversion efficiency is defined as the probability for a neutron to produce a charged particle coming out of the coating layer. As shown in Fig. 2, the conversion efficiency increases linearly with the <sup>238</sup>U coating thickness firstly, then decreases as the thickness increases. the efficiency decreases since the produced charged particles are stopped in the foil. Fission fragments, all heavy fragments, can almost be detected by the PPAC as long as they are not stopped in the coating layer. Therefore, the conversion efficiency here can be regarded as the detection efficiency of the detector.

This simulation results could provide a design reference for the optimal thickness of coating layer in the experiment. By considering the conversion efficiency and electroplating technological level, we chose to electroplate 300 μg/cm<sup>2</sup> <sup>238</sup>U(U<sub>3</sub>O<sub>8</sub>) on both sides of a 30 μm thick Ti backing to ensure the acceptable uniformity of the coating at such target thickness. The simulation results of

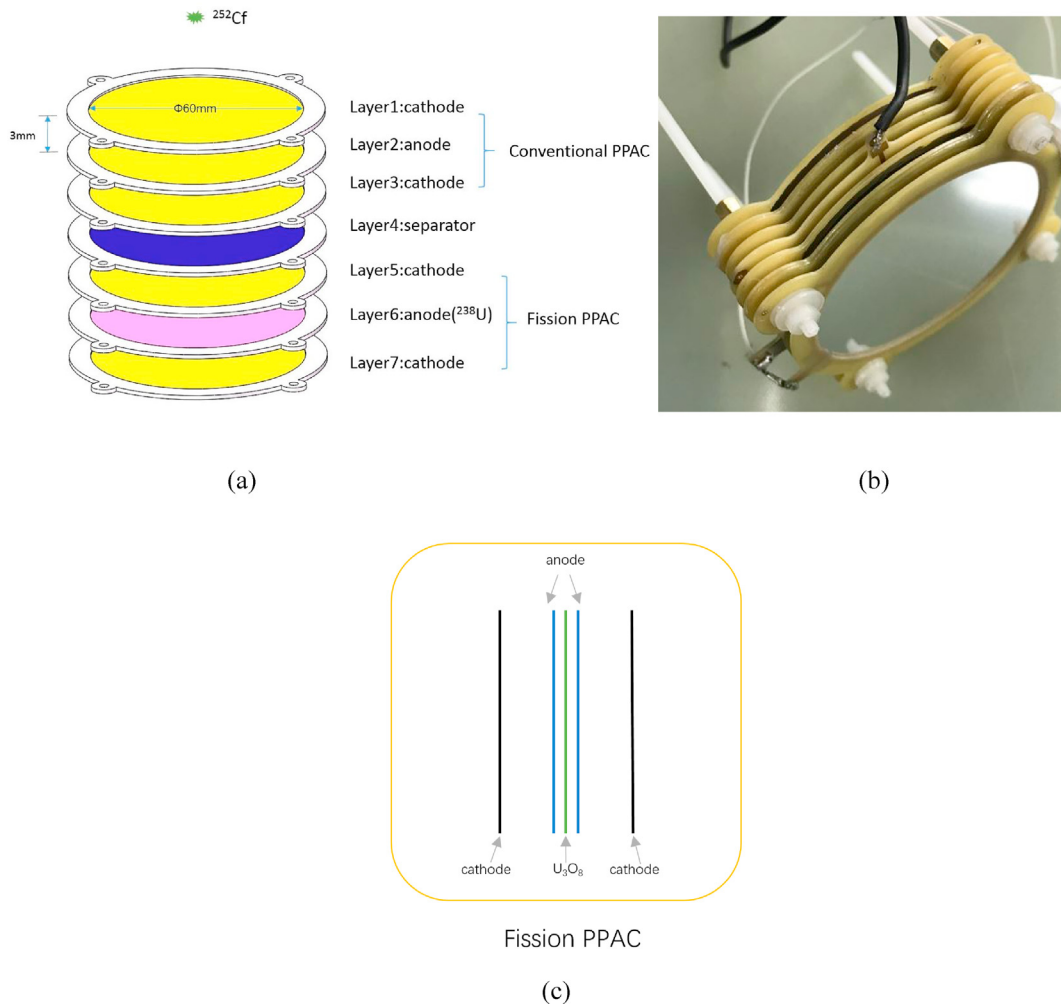
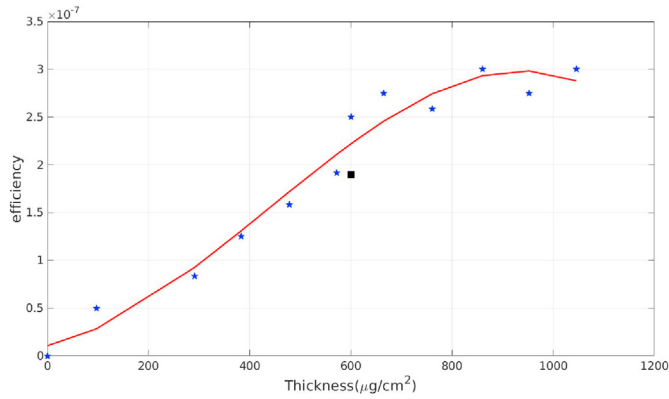


Fig. 1. (a) provides a schematic view of the Dual-PPACs. Layers 1–3 are the three electrodes of the conventional PPAC, and layers 5–7 are the fission PPAC. U<sub>3</sub>O<sub>8</sub> target is attached at the anode of the fission PPAC. Layer 4 is the separator. (b) is a photo of the Dual-PPACs we used in this work. (c) is a schematic view of the fission PPAC.



**Fig. 2.** Evolution of the efficiency of fission fragments detection with the thickness of  $^{238}\text{U}$  coating. The star dot fitted by the red line are the results obtained with Geant4 simulation. The square stands for experimental result. (For interpretation of the references to colour in this figure legend, the reader is referred to the Web version of this article.)

conversion efficiency, given the thickness measurement of  $600\ \mu\text{g}/\text{cm}^2$ , which reaches  $2.5 \times 10^{-7}$ , are in good agreement with our experimental results ( $1.9 \times 10^{-7}$ , square).

### 3. Test and performance

A  $^{252}\text{Cf}$  source was conducted to examine the performance of the Dual-PPACs, including TOF measurement and the energy deposit measurement of spontaneous fission products of  $^{252}\text{Cf}$ . Current neutron emissivity of  $^{252}\text{Cf}$  source is  $1.3 \times 10^5\ \text{n/s}$ , the active area is  $\Phi 10\text{mm}$ . In order to minimize uncertainties, the distance between the  $^{252}\text{Cf}$  source and the first layer of the detector is 1.5 cm in order to cover a solid angle as large as possible. The Dual-PPACs detector and the  $^{252}\text{Cf}$  source were encapsulated in an aluminum cylindrical tank filling with flowing gas  $\text{C}_4\text{H}_{10}$ . In this work, the anode was connected to high voltage, while the cathodes received the signals. And the different voltage was applied while gas pressure changes, for the purpose of getting the relationship between detection efficiency and voltage accurately.

#### 3.1. Energy deposition measurement

To obtain a suitable range of operating voltage, we performed the energy deposition measurement of the fission products of  $^{252}\text{Cf}$  (spontaneous fission fragments and  $\alpha$ ) using the conventional PPAC. Fig. 3 provides the data acquisition schematic used in

laboratory tests. The signal obtained from cathodes of conventional PPAC is split into fast timing signals and energy signals. The energy signals are amplified by the ORTEC 572A amplifier and transmitted to the ADC. The fast timing signals are amplified by Fast Timing Amplifiers (FTA810, ORTEC) with a gain of 200. Signals out from FTA are discriminated by Constant-Fraction Discriminators (CF8000, ORTEC) and are sent to the TDC.

To remove  $\alpha$  particle induced signal, noise and other effects, a certain threshold is always required to set in the Constant-Fraction Discriminators (CF8000, ORTEC). In order to get the performances of the detector under different high voltages, we changed the voltages with a step of 10V at 6 mbar or 10 mbar gas pressures, as shown in Fig. 4. The measured results provided an experimental reference to the optimum voltage for the given gas pressure, and these parameters were selected for subsequent timing

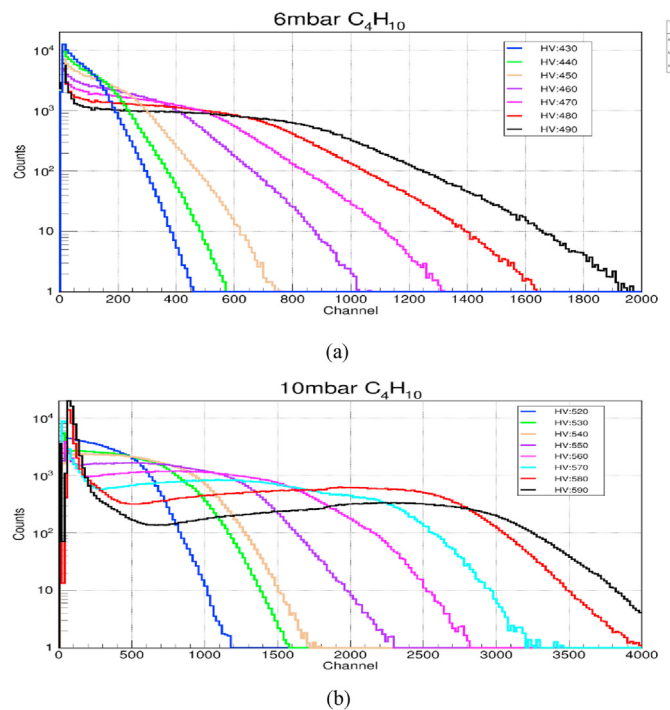


**Fig. 4.** (a) The calibrated energy spectrum of spontaneous fission products at 6 mbar  $\text{C}_4\text{H}_{10}$ . The reduced electric field varied from 215V/cm/mbar to 245V/cm/mbar. (b) The calibrated energy spectrum of spontaneous fission products at 10 mbar  $\text{C}_4\text{H}_{10}$ . The reduced electric field varied from 156V/cm/mbar to 177V/cm/mbar. The counts in the ordinate are expressed in logarithmic form.

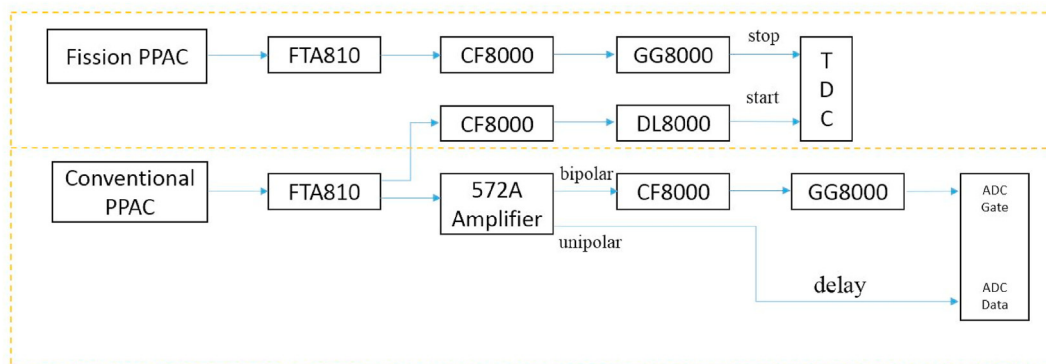


**Fig. 3.** The electronic block diagram of the test. The data obtained by ADC is for the energy deposit measurement of spontaneous fission products of  $^{252}\text{Cf}$ , while the data obtained by TDC is for the TOF measurement.

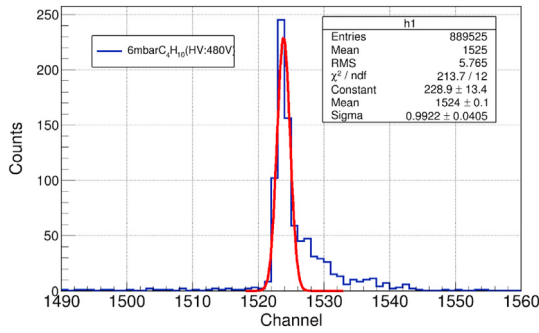


Fig. 5. The measured timing spectrum between the conventional PPAC and the fission PPAC under the optimal time resolution. Each channel on the abscissa corresponds to a time interval of 0.1 ns.

measurement. In our experiment, the conventional PPAC and the fission PPAC are considered to have the same timing property, which can be verified in this way. The analog signals of these two PPACs amplified by FTA810 were monitored through oscilloscope during the test, and the analog signals of the fission PPAC were consistent with those of the conventional PPAC.

### 3.2. Timing-property measurement

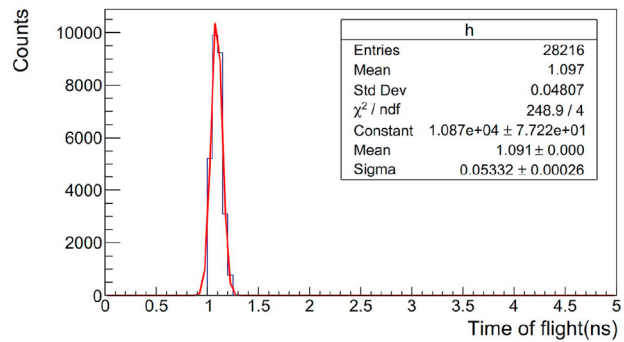
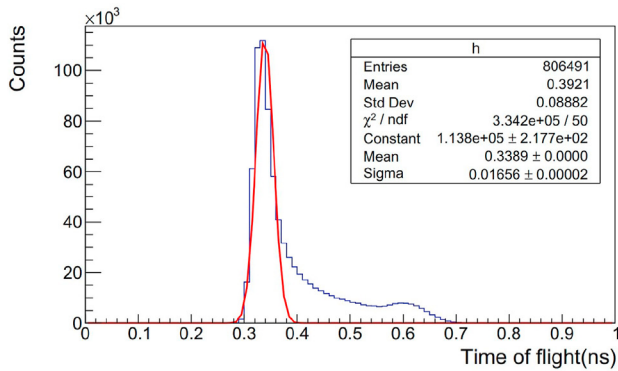
The following steps briefly describe the principle of timing-property measurement. The  $^{252}\text{Cf}$  source simultaneously emits spontaneous fission fragments and neutrons. The neutrons, pass through the conventional PPAC, induce the nuclear fission reaction

with  $^{238}\text{U}(\text{U}_3\text{O}_8)$  coating in the fission PPAC. Two complementary fission fragments are emitted in opposite directions. But the  $\text{U}_3\text{O}_8$  target is electroplated on both sides of the Ti backing. It is impossible to measure the two fragments in a fission event at both cathodes of the fission PPAC because fragments cannot penetrate the backing. Fission fragments are all heavy, can almost be detected by the PPAC as long as they are not stopped in the coating. Conventional PPAC could detect outgoing spontaneous fission fragments. When the spontaneous fission fragment was detected by conventional PPAC and the neutron was detected through fission PPAC, two signals from two PPACs were transmitted into the acquisition(TDC). The signal from conventional PPAC by spontaneous fission fragment is set as the starting time, the signal from fission PPAC by a neutron is taken as the stopping time correspondingly, as shown in Fig. 3. The two coincident signals of two adjacent PPACs identified the fission events.

Fig. 5 shows the measured timing spectrum between the conventional PPAC and the fission PPAC under the optimal time resolution. Each channel on the abscissa corresponds to a time interval of 0.1 ns. The peak FWHM is 0.23 ns. The timing spectrum can be express as

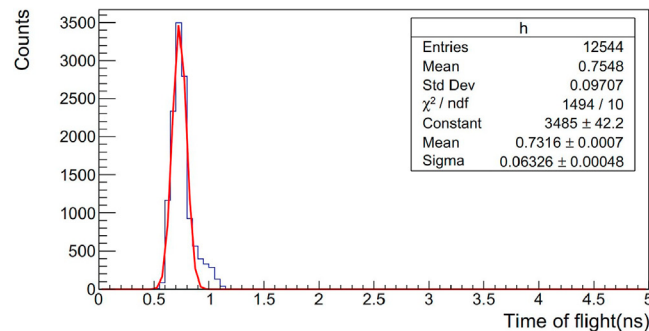
$$\sigma_{\text{exp}}^2 = \sigma_n^2 + \sigma_f^2 + \sigma_{\text{TOFn}}^2 + \sigma_{\text{TOFf}}^2 \quad (1)$$

Where  $\sigma_{\text{exp}}^2$  is the standard deviation of the timing spectrum in the experiment.  $\sigma_n^2$  represents the intrinsic time resolution for the fission PPAC;  $\sigma_f^2$  represents the intrinsic time resolution for the conventional PPAC;  $\sigma_{\text{TOFn}}^2$  is the relative uncertainty of the time of flight of neutrons and  $\sigma_{\text{TOFf}}^2$  is the relative uncertainty of the time of flight of spontaneous fission fragments.



(a)

(b)



(c)

Fig. 6. The TOF spectrum for spontaneous fission fragments (a) and neutrons (b) obtained with Geant4 simulation. (c) the time difference spectrum between neutrons and spontaneous fission fragments.

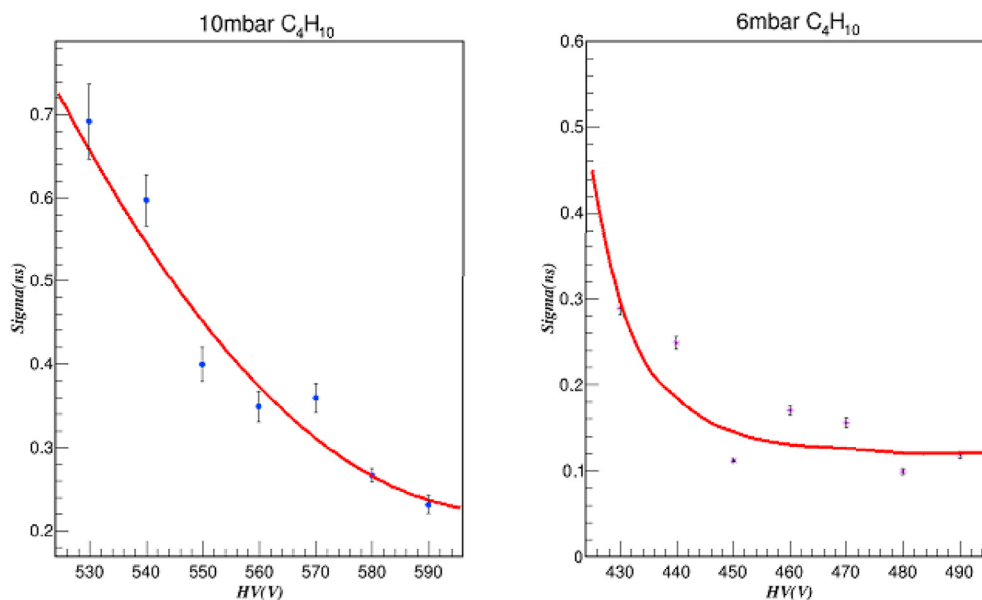


Fig. 7. The sigma, which indicates the time resolution of PPACs, is a function of the high voltage applied on the anode. The blue points represent the experimental data with statistical error bars. The red line serves as the fitting of the data. (For interpretation of the references to colour in this figure legend, the reader is referred to the Web version of this article.)

We performed the Dual-PPACs detector simulation based on the Geant4 MC code to obtain the timing spectra of neutrons and spontaneous fission fragments. A simplified model was established in Geant4 simulation, which consists of two PPACs and the  $^{238}\text{U}$  target attached to fission PPAC to increase the consistency with the experiments. The simulated  $^{252}\text{Cf}$  resource's energy spectrum is described as a Maxwell-like distribution, and neutrons are emitted with an angular distribution. The simulation results are shown in Fig. 6.  $\sigma_{\text{TOFn}}$  is about to 53 ps and  $\sigma_{\text{TOFf}}$  is about to 16 ps.  $\sigma_{\text{TOFn}}^2$  and  $\sigma_{\text{TOFf}}^2$  contribute little to the timing spectrum, which can be almost negligible. Fission PPAC and conventional PPAC detect fission fragments with similar energy and have negligible gain difference at the plateau region in Fig. 7. The intrinsic time resolution of these two PPACs can be regarded as the same here. The coincidence of the two PPACs' time resolution indicates that the time resolution of the Dual-PPACs detector is 164ps.

From channels 1530 to 1540 in Fig. 5, the timing spectrum has some disorderly count that forms a short tail. According to the simulation results in Fig. 6, the time difference spectrum between the neutron and the spontaneous fission fragment was obtained by taking the signal time of the spontaneous fission fragments as the starting signal, which has a time distribution spectrum with a tail similar to that measured in the experiment. It can be deduced that there are two main reasons for the tail formation of the measured timing spectrum. One is a right tail by the low-energy fission fragments on the timing spectrum due to the long flight time. The energy of spontaneous fission fragments is from 50 MeV to 120 MeV. Another reason is the large thickness of the  $^{252}\text{Cf}$  source used in our experiment. Spontaneous fission fragments may lose most of their energy in the source at a large emission angle, and these low-energy fragments will also create a timing spectrum tail.

In timing-property measurement experiment, we established the same working conditions as the energy deposit measurement above. It is worth noting in Fig. 7 that the sigma of the time resolution changes with the high voltage applied on the anode. As the anode voltage increases, the time resolution relatively improves, finally reaches the plateau region. The detector begins to spark when the voltage higher than 590V at 10 mbar. The overall time

resolution at 6 mbar is better than that at 10 mbar. When the gas pressure is 6 mbar, and anode voltage is 480V, the time resolution is at its optimal level, as shown in Fig. 5.

#### 4. Conclusion

We developed a Dual-PPACs detector for fast neutron measurements, which consists of two distinctive sets, namely conventional and fission PPACs. Each PPAC consists of one anode and two cathodes.  $\text{A}^{238}\text{U}(\text{U}_3\text{O}_8)$  coating is placed in the anode of the fission PPAC. the  $^{252}\text{Cf}$  spontaneous fission source was adopted to measure both the Dual-PPACs detector's detection efficiency and time resolution. The detection efficiency was estimated to be  $1.9 \times 10^{-7}$ , consistent with the efficiency of  $2.5 \times 10^{-7}$  given by a Geant4 simulation. An excellent time resolution of 164ps was observed at 6 mbar in isobutene gas. The results indicate that the Dual-PPACs has great performance in fast neutron measurements.

#### Declaration of competing interest

The authors declare that they have no known competing financial interests or personal relationships that could have appeared to influence the work reported in this paper.

#### Acknowledgments

This work is financially supported by National Key R&D Program of China (Grant No. 2018YFE0205200), the National Natural Science Foundation of China (Grant No. U1432123, 11575268, 11875174, 11875301, 11675238).

#### References

- [1] J. Christiansen, G. Hempel, H. Ingwersen, Investigation of delayed fission in  $^{236}\text{U}$ , Nucl. Phys. 239 (1975) 253–259.
- [2] e. a F. H. G. Hempel, G. Schatz, Development of parallel-plate avalanche counters for the detection of fission fragments, Nucl. Instrum. Methods 131 (1975) 445–450.
- [3] H. Stelzer, A large area parallel plate avalanche counter, Nucl. Instrum. Methods 133 (1976) 409–413.

- [4] A. Breskin, N. Zwing, Timing properties of parallel plate avalanche counters with light particles, *Nucl. Instrum. Methods* 144 (1977) 609–611.
- [5] J.C. Sanabria, B.L. Berman, C. Cetina, Parallel-plate avalanche detectors with anode wire grids, *Nucl Phys A* 441 (2000) 525–534.
- [6] H. Kumagai, T. Ohnishi, Development of parallel plate avalanche counter (PPAC) for BigRIPS fragment separator, *Nucl. Instrum. Methods Phys. Res. B* 317 (2013) 717–727.
- [7] C.Y. Wu, R.A. Henderson, A multiple parallel-plate avalanche counter for fission-fragment detection, *Nucl. Instrum. Methods Phys. Res. A* 794 (2015) 76–79.
- [8] Xianglun Wei, Fenhai Guan, Herun Yang, Development of Parallel Plate Avalanche Counter for heavy ion collision in radioactive ion beam, *Nucl. Eng. Technol.* 52 (3) (2020) 575–580.
- [9] S. A. Geant4 - a simulation toolkit, *Nucl. Instrum. Methods Phys. Res. A* 506 (2003) 250–303.
- [10] J. A. Geant4 developments and applications, *IEEE Trans. Nucl. Sci.* 53 (2006) 270–278.